

On the free energy of ionic hydration

Gerhard Hummer,^{*ab} Lawrence R. Pratt,^c and Angel E. García^a
(April 6, 1995)

The Journal of Physical Chemistry (in press, 1995)

The hydration free energies of ions exhibit an approximately quadratic dependence on the ionic charge, as predicted by the Born model. We analyze this behavior using second-order perturbation theory. This provides effective methods to calculating free energies from equilibrium computer simulations. The average and the fluctuation of the electrostatic potential at charge sites appear as the first coefficients in a Taylor expansion of the free energy of charging. Combining the data from different charge states (*e.g.*, charged and uncharged) allows calculation of free-energy profiles as a function of the ionic charge. The first two Taylor coefficients of the free-energy profiles can be computed accurately from equilibrium simulations; but they are affected by a strong system-size dependence. We apply corrections for these finite-size effects by using Ewald lattice summation and adding the self-interactions consistently. An analogous procedure is used for reaction-field electrostatics. Results are presented for a model ion with methane-like Lennard-Jones parameters in SPC water. We find two very closely quadratic regimes with different parameters for positive and negative ions. We also studied the hydration free energy of potassium, calcium, fluoride, chloride, and bromide ions. We find negative ions to be solvated more strongly (as measured by hydration free energies) compared to positive ions of equal size, in agreement with experimental data. We ascribe this preference of negative ions to their strong interactions with water hydrogens, which can penetrate the ionic van der Waals shell without direct energetic penalty in the models used. In addition, we consistently find a positive electrostatic potential at the center of uncharged Lennard-Jones particles in water, which also favors negative ions. Regarding the effects of a finite system size, we show that even using only 16 water molecules it is possible to calculate accurately the hydration free energy of sodium if self-interactions are considered.

^a Address for Correspondence: Theoretical Biology and Biophysics Group T-10, MS K710, Los Alamos National Laboratory, Los Alamos, New Mexico 87545

FAX: (505) 665-3493; Phone: (505) 665-1923; E-mail: hummer@t10.lanl.gov

^b Center for Nonlinear Studies, Los Alamos National Laboratory, MS B258, Los Alamos, New Mexico 87545

^c Theoretical Chemistry and Molecular Physics Group T-12, MS B268, Los Alamos National Laboratory, Los Alamos, New Mexico 87545

I. INTRODUCTION

A *quadratic* dependence on the ionic charge of the electrostatic free energy of solvation of a simple ion in aqueous solution is about the simplest reasonable possibility for that behavior. The Born model predicts that quadratic dependence.¹ Several computer simulation calculations have shown that it is approximately correct for the simplest monovalent ions in water.^{2–4} Theoretical simplifications have been advanced to take advantage of such behavior.^{3,5–7}

If that quadratic behavior were correct with sufficient accuracy, it would indeed permit important simplifications of the difficult task of molecular calculations of solvation free energies owing to electrostatic interactions in complex solutions. The theoretical simplifications identified on that basis can be viewed either as perturbation theory through second order in the electrostatic interactions, or as a Gaussian modeling of certain thermal fluctuations of those interactions. Adopting either view, these methods would have wide applicability and great simplicity. The question of the accuracy of the quadratic dependence on charge of the free energy owing to electrostatic interactions deserves to be raised for its own sake and given a precise answer as general as possible.

This quadratic behavior is not a universal truth and previous simulation calculations have given helpful information on the circumstances where this quadratic dependence can be expected to fail.² However, previous simulation calculations are sufficiently disparate that a high precision answer to the question of the accuracy of second-order perturbation theory for the free energy owing to electrostatic interactions is not available. The disparate character of the available simulation results is largely caused by a lack of uniformity with respect to the treatment of finite-system-size effects on electrostatic interactions in aqueous solutions. It is not atypical for a finite-system-size correction and the electrostatic solvation free energy to be of similar size.

In contrast to the role of computer experiments in answering this question, laboratory experiments have been useful mostly for framing the question.^{8–10} The difficulty of using laboratory experiments for the present purpose resides in our inability to extract generally an electrostatic contribution from contributions of the other interactions present.

Because of these points, this work calculates the free energy owing to electrostatic interactions of simple, spherical ions in water by Monte Carlo methods and gives particular attention to the methodological issue of correction for finite system size. The molecular models used are simple but they have been widely tested. Because the goal of this work is to address the question of quadratic dependence on charge of the electrostatic solvation free energy, these models are sufficiently realistic for the present purposes. However, we will compare our computed free energies with experimental results and thus provide information on how these models might be simply improved for prediction of electrostatic free energies.

Before proceeding with the technical developments it is worthwhile to give some discussion of the idea for the present treatment of system-size effects on solvation free energies of ions. There is no generally valid recipe that allows a determination of the effects of a finite system size on the calculated physical quantity in computer simulations. What must generally be done is to analyze the observed size dependence empirically. If, as is the case for Coulomb interactions of long range, different procedures are available, then we should expect consistent thermodynamic limiting ($N \rightarrow \infty$) results for different methods of treating the finite-size system. It is well understood that certain quantities involving integrals over the whole sample, such as the dipole-moment fluctuations, depend intrinsically on exterior conditions or constraints.¹¹ Those conditions must then be properly understood theoretically.

For the present problem involving the interactions and associated thermodynamics of an ion immersed in a dielectric liquid, a reasonable view is the following: Treatment of electrostatic interactions in a truly periodic format, *e.g.*, by Ewald procedures, is consistent with the periodic boundary conditions that are nearly inevitable for other reasons. In periodic boundary conditions the interactions at the longest range that *must* be taken seriously occur at an appreciable fraction of the distance to the surface of the simulation cell. For typical simulated system sizes, ionic interactions at that longest range are large. Treatment of electrostatic interactions in a truly periodic format thoroughly tempers those large interactions. But a mathematical price for true periodicity of electrostatic interactions is a “self-interaction” associated with interactions with images and a uniform neutralizing charge background. For neutral systems this self-interaction can be sometimes ignored. For non-neutral systems such as those studied here there may be practical advantages of consistency obtained for explicit consideration of the self-interaction. We will account for these self-interactions explicitly in the calculations below.

This argument permits treatments of the ionic interactions other than Ewald summation. In fact, the work below tests a generalized reaction-field (GRF) method and also finds that consistent results can be obtained if self-interactions are treated on a similar basis.

II. THEORETICAL METHODS

A. Calculation of the free energy of charging

The various methods to compute free energies using computer simulations have been reviewed extensively.^{12–14} We start here from the potential distribution theorem for the excess chemical potential μ^{ex} ,¹⁵

$$\mu^{ex}(q_1) - \mu^{ex}(q_0) = -k_B T \ln \langle \exp \{ -\beta [u(q_1) - u(q_0)] \} \rangle_{q_0} , \quad (1)$$

where q_0 and q_1 are the two charge states and $\beta = 1/k_B T$; $\langle \dots \rangle_q$ denotes a thermal configuration-space average in the charge-state q ; and $u(q)$ is the configuration-dependent interaction energy of the ion in charge-state q with the solution. Apart from finite-size corrections to be discussed later, $u(q)$ is given by $q\phi(\mathbf{r})$, where $\phi(\mathbf{r})$ is the electrostatic potential at the charge position \mathbf{r} .

We next analyze eq 1 utilizing a cumulant expansion¹⁶ with respect to β ,

$$\langle \exp(-\beta \Delta u) \rangle_{q_0} = \exp \left[\sum_{n=0}^{\infty} (-\beta)^n \frac{C_n}{n!} \right] , \quad (2)$$

where $\Delta u = u(q_1) - u(q_0)$. This defines the cumulants C_n of order $n = 0, 1, 2$ as

$$C_0 = 0 \quad (3a)$$

$$C_1 = \langle \Delta u \rangle_{q_0} \quad (3b)$$

$$C_2 = \left\langle \left(\Delta u - \langle \Delta u \rangle_{q_0} \right)^2 \right\rangle_{q_0} . \quad (3c)$$

We can interpret eq 2 as a Taylor expansion in $\Delta q = q_1 - q_0$ if we set $\Delta u = \Delta q\phi + (q_1^2 - q_0^2)\xi/2$, where ξ accounts for finite-size effects as a “self-interaction” to be discussed further below,

$$\Delta\mu^{ex} = \Delta q \left(\langle \phi \rangle_{q_0} + q_0 \xi \right) - \frac{\beta}{2} \Delta q^2 \left[\left\langle \left(\phi - \langle \phi \rangle_{q_0} \right)^2 \right\rangle_{q_0} - \frac{\xi}{\beta} \right] + \dots , \quad (4)$$

where $\Delta\mu^{ex} = \mu^{ex}(q_1) - \mu^{ex}(q_0)$. The mean and the fluctuation of the electrostatic potential at the charge site q (corrected for finite-size effects) yield the derivatives of the free energy with respect to Δq . The information about the derivatives can therefore be extracted from equilibrium simulations. In principle, higher-order cumulants could be used to obtain information about the other Taylor coefficients. However, as was observed by Smith and van Gunsteren,⁴ higher-order cumulants are increasingly difficult to extract from computer simulations of limited duration.

Therefore, we will evaluate C_1 and C_2 at few discrete charge states and combine this information about the derivatives, either by constructing an interpolating polynomial or by using a χ^2 fit to a polynomial expression (or any other functional form) for the free energy as a function of Δq . The χ^2 fit minimizes the mean square deviation of the observed data with respect to the coefficients $\{a_k\}$ of the fitting function $\Delta\mu^{ex}(q; \{a_k\})$,

$$\chi^2 = \sum_{i=1}^n \left\{ \left[\frac{\Delta\dot{\mu}^{ex}(q_i; \{a_k\}) - \Delta\dot{\mu}_{\text{obs}}^{ex}(q_i)}{\sigma_i} \right]^2 + \left[\frac{\Delta\ddot{\mu}^{ex}(q_i; \{a_k\}) - \Delta\ddot{\mu}_{\text{obs}}^{ex}(q_i)}{\rho_i} \right]^2 \right\} , \quad (5)$$

where σ_i and ρ_i are the estimated errors (standard deviations) of the observed first and second derivatives $\dot{\mu}_{\text{obs}}^{ex}$ and $\ddot{\mu}_{\text{obs}}^{ex}$ at charge-state q_i .

B. Long-range Coulomb interactions and finite-size effects

To minimize finite-size effects on energetic properties of Coulombic systems, we adopt the following strategy:¹⁷ We use lattice summation for calculating the electrostatic interactions to account for the periodic boundary conditions employed in the computer simulations; and we consistently include the self-interactions arising from lattice summation. We point out that aside from formal consistency the numerical results can motivate this approach by demonstrating in a finite-size analysis that the deviations from the thermodynamic limit ($N \rightarrow \infty$) are small.

The Coulomb energy of a periodically replicated system of charges q_i at positions \mathbf{r}_i ($i = 1, \dots, N$) can be expressed as

$$U = \sum_{1 \leq i < j \leq N} q_i q_j \varphi_{\text{EW}}(\mathbf{r}_{ij}) + \frac{1}{2} \sum_{1 \leq i \leq N} q_i^2 \xi_{\text{EW}} , \quad (6)$$

where $\mathbf{r}_{ij} = \mathbf{r}_j - \mathbf{r}_i + \mathbf{n}$, with the lattice vector \mathbf{n} chosen such that \mathbf{r}_{ij} is a vector in the unit cell. The effective, position-dependent potential $\varphi_{\text{EW}}(\mathbf{r})$ is obtained by lattice summation using Ewald's method,^{13,18,19}

$$\varphi_{\text{EW}}(\mathbf{r}) = \sum_{\mathbf{n}} \frac{\text{erfc}(\eta|\mathbf{r} + \mathbf{n}|)}{|\mathbf{r} + \mathbf{n}|} + \sum_{\mathbf{k} \neq 0} \frac{4\pi}{V k^2} \exp\left(-\frac{k^2}{4\eta^2} + i\mathbf{k} \cdot \mathbf{r}\right) - \frac{\pi}{V\eta^2} , \quad (7)$$

where V is the volume of the box, erfc is the complementary error function, and $k = |\mathbf{k}|$. The two lattice sums extend over real- and Fourier-space lattice-vectors \mathbf{n} and \mathbf{k} , respectively.

The self term $\xi_{\text{EW}} = \lim_{\mathbf{r} \rightarrow 0} [\varphi_{\text{EW}}(\mathbf{r}) - 1/r]$ is the Wigner potential:^{20–22} Using Green's theorem and $\Delta(1/r) = -4\pi\delta(\mathbf{r})$, we find

$$\xi_{\text{EW}} = \lim_{\mathbf{r} \rightarrow 0} \left[\varphi_{\text{EW}}(\mathbf{r}) - \frac{1}{r} \right] = -\frac{1}{4\pi} \lim_{\epsilon \rightarrow 0} \int_{|\mathbf{r}| > \epsilon} d\mathbf{r} \frac{1}{r} \Delta\varphi_{\text{EW}}(\mathbf{r}) . \quad (8)$$

The integration region is infinite and includes all background charge and lattice image charges,

$$\Delta\varphi_{\text{EW}}(\mathbf{r}) = -4\pi \sum_{\mathbf{n}} \left[\delta(\mathbf{r} - \mathbf{n}) - \frac{1}{V} \right] . \quad (9)$$

Eqs 8 and 9 establish that ξ_{EW} is the electrostatic potential in a Wigner lattice at a charge site owing to the lattice images and the neutralizing background. For Ewald summation in a cubic lattice the self term is $\xi_{\text{EW}} = -2.837297/L$,^{21–23} where L is the length of the cube.

It will be interesting to remember that ξ_{EW} can also be expressed in terms of quantities associated with the primitive simulation cell

$$\xi_{\text{EW}} = -\frac{1}{4\pi} \lim_{\epsilon \rightarrow 0} \int_{V:|\mathbf{r}| > \epsilon} d\mathbf{r} \frac{1}{r} \Delta\varphi_{\text{EW}}(\mathbf{r}) - \frac{1}{4\pi} \int_{\partial V} d^2 r \varphi_{\text{EW}}(\mathbf{r}) \hat{\mathbf{n}} \cdot \nabla \left(\frac{1}{r} \right) . \quad (10)$$

The first term on the right is explicitly the interaction with the background density in the primitive simulation cell. The second term on the right is an integral over the surface of the primitive simulation cell. It describes electrostatic interactions of the central unit charge with a dipolar surface distribution $\varphi_{\text{EW}}(\mathbf{r}) \hat{\mathbf{n}}$, where $\hat{\mathbf{n}}$ is the surface normal pointing outwards.

Eq 6 can also be used for a non-neutral system since charges are implicitly compensated by a homogeneous background in the Ewald formulation. This results in an expression for the energy difference Δu between two configurations with different charge-states q_0 and q_1 of an ion at position \mathbf{r} ,

$$\Delta u = \Delta q \varphi_{\text{EW}}(\mathbf{r}) + \frac{1}{2} \xi_{\text{EW}} (q_1^2 - q_0^2) . \quad (11)$$

In the following, we will use this expression containing a self-interaction which is quadratic in the charge to calculate the free energy of charging; *i.e.*, we assume that the self-interaction accounts for the finite-size corrections.²⁴

In our calculations, we will also use a generalized reaction field (GRF).^{25,26} The GRF Coulomb interaction depends only on the distance r of the charges and has a cutoff-distance r_c ,

$$\varphi_{\text{GRF}}(r) = \frac{1}{r} p(r/r_c) \Theta(r_c - r) + C . \quad (12)$$

Θ is the Heaviside unit-step function; $p(x)$ is a screening polynomial:

$$p(x) = (1 - x)^4 (1 + 8x/5 + 2x^2/5) . \quad (13)$$

By analogy with Ewald summation, we define the self term for the GRF as the potential at the charge site, $\xi_{\text{GRF}} = \lim_{\mathbf{r} \rightarrow 0} [\varphi_{\text{GRF}}(\mathbf{r}) - 1/r]$. The total energy of neutral systems, if defined as in eq 6, is independent of the constant C . However, in non-neutral systems C affects the total energy. We define C in analogy with the Ewald potential, which satisfies²²

$$\int_V d\mathbf{r} \varphi_{\text{EW}}(\mathbf{r}) = 0 , \quad (14)$$

such that the average potential in the cell vanishes. If we require the normalization condition eq 14 also for the GRF interaction, we obtain $C = -\pi r_c^2/5V$. The GRF self term is $\xi_{\text{GRF}} = -12/5r_c + C$. For $r_c = L/2$, the normalization condition eq 14 accounts for only a small additional correction yielding $\xi_{\text{GRF}} = -24/5L - \pi/20L$.²⁷

It is interesting to make a connection with the correction method proposed by Sloth and Sørensen.²⁷ These authors use the minimum-image Coulomb interaction. To eliminate the system-size dependence in their calculation of chemical potentials of restricted-primitive-model ions, they introduce a background neutralizing the test-particle charge. This is done by adding a constant $\xi_{1/r}$ to the bare Coulomb potential,²⁸

$$\xi_{1/r} = -\frac{1}{V} \int_V d\mathbf{r} \frac{1}{r} . \quad (15)$$

This corresponds to enforcing eq 14 and adding a self term $\xi_{1/r} = \lim_{r \rightarrow 0} [\varphi(r) - 1/r]$ for the minimum-image interaction. $\xi_{1/r}$ is also precisely the first term on the right side of eq 10. It accounts for a large correction since $\xi_{1/r} \approx -2.38/L$.

III. COMPUTER SIMULATIONS

We calculated the free energy of charging ions in water using Metropolis Monte Carlo simulations.^{13,30} The systems comprise a single ion and N water molecules. For water we used the simple point charge (SPC) model.³¹ The ion-water interactions were described by Coulomb and Lennard-Jones (LJ) interactions. The Coulomb terms involve the partial charges of oxygens and hydrogens on SPC water. The LJ interactions act only between water oxygen and the ion. We studied the ions Na^+ , K^+ , Ca^{2+} , F^- , Cl^- , and Br^- . The LJ parameters for these ions were those of Straatsma and Berendsen.³² We also studied the charging of a model ion Me with methane LJ parameters as given by Jorgensen *et al.*³³ Lorentz-Berthelot mixing rules¹³ were applied to obtain LJ parameters between water and Me. The LJ parameters are compiled in Table I.

The charge interactions in the simulations were calculated using Ewald lattice summation (eqs 6 and 7) and the generalized reaction-field potential (eqs 12 and 13). In both cases, the real-space interactions were truncated on an atom basis using $L/2$ as cutoff and applying the periodic boundary conditions on an atom basis. For the Ewald Fourier-space calculation, a cutoff $k^2 \leq 38(2\pi/L)^2$ was used resulting in $2 \times 510 \mathbf{k}$ vectors. To correct the background dielectric constant from infinity to $\epsilon_{\text{RF}} = 65$, a term $2\pi\mathbf{M}^2/(2\epsilon_{\text{RF}} + 1)V$ was added to the potential energy (in both Ewald and GRF calculations), where \mathbf{M} is the net dipole moment of the water molecules. The real-space damping factor was set to $\eta = 5.6/L$. Electrostatic potentials at the ion sites were calculated using φ_{EW} and φ_{GRF} . The potentials were calculated after each pass (one attempted move per particle) and stored for analysis. For each system 100 000 passes were used for averaging. Random configurations or configurations of previous runs were used as initial structures and always extensively equilibrated. The temperature was 298 K. The total number density was $\rho = 33.33 \text{ nm}^{-3}$ in all simulations. Cubic boxes were used as simulation cells with edges $L = [(N + 1)/\rho]^{1/3}$. The Monte Carlo move widths were chosen so that an approximate acceptance ratio of 0.5 was obtained.

In addition, thermodynamic integration (TI) was used to calculate directly the free energy of charging. Within 100 000 Monte Carlo passes, the charge of the ion was linearly changed from 0 to its full magnitude ($\pm e$, $2e$, where e is the elementary charge). The free-energy changes were then calculated as

$$\mu^{ex}(q_1) - \mu^{ex}(q_0) = (q_1 - q_0)n^{-1} \sum_{i=1}^n \phi_i + \xi(q_1^2 - q_0^2)/2 , \quad (16)$$

where the sum extends over $n = 100\,000$ Monte Carlo passes and the last term is a finite-size correction. Eq 16 approximates the exact expression

$$\mu^{ex}(q_1) - \mu^{ex}(q_0) = \int_{q_0}^{q_1} dq \left\langle \frac{\partial u(q)}{\partial q} \right\rangle_q . \quad (17)$$

TI was also performed using the reverse path, *i.e.*, decreasing the charge to 0.

We also performed Monte Carlo simulations of ion-water clusters comprising one ion and N SPC water molecules ($4 \leq N \leq 256$). The starting structure was a random configuration with bulk density of water in a cubic box around the ion. The cluster was equilibrated for at least 50 000 passes (with an acceptance rate of about 0.5) and then averaged over 50 000 passes at 298 K. We used the bare Coulomb interaction $1/r$ and did not apply a distance cutoff. No periodic boundary conditions were employed in the cluster simulations.

IV. RESULTS AND DISCUSSION

A. Charging of a methane-like Lennard-Jones particle

The free energy of charging a methane-like LJ particle in SPC water was determined from a series of simulations with $N = 128$ and 256 water molecules and with Ewald and GRF charge treatment. A range of charges from $-e$ to e was covered in steps of $0.25e$ ($N = 128$) and $0.5e$ ($N = 256$). The results for the mean m and the fluctuation f of the potential at the ion site (with and without finite-size correction) are compiled in Table II. In the calculations, the potential ϕ at the ion site ($\mathbf{r}=0$) is defined as

$$\phi = \sum_{i=1}^N \sum_{\alpha=1}^3 q_{i\alpha} \varphi(\mathbf{r}_{i\alpha}) , \quad (18)$$

where the double sum extends over all water oxygen and hydrogen sites; φ is either φ_{EW} or φ_{GRF} . The mean m and the fluctuation f are calculated from 100 000 Monte Carlo passes as

$$m = e\langle\phi\rangle , \quad (19a)$$

$$f = \beta e^2 \langle(\phi - \langle\phi\rangle)^2\rangle . \quad (19b)$$

The corrected values for mean and fluctuation are defined as $m_c = m + qe\xi$ and $f_c = f - e^2\xi$. The Taylor expansion of the free energy of charging around a charge-state q assumes the following form:

$$\Delta\mu^{ex} = \left(\frac{\Delta q}{e}\right) m_c - \frac{1}{2} \left(\frac{\Delta q}{e}\right)^2 f_c + \dots . \quad (20)$$

From the results of Table II we see that the finite-size corrections are of similar magnitude as the uncorrected results m and f . The uncorrected results of the different methods and system sizes are widely spread. If however the finite-size corrections are applied, we obtain consistent results for all methods and system sizes over the range of ion charges considered. With estimated errors (one standard deviation, as calculated from block averages) of 4.0 and 30 kJ mol $^{-1}$ for m_c and f_c , we find data of different methods within two standard deviations from each other. The only exception is the fluctuation f_c for $q = -e$, where the two extreme values (Ewald, $N = 128$ and 256) differ by about three standard deviations. In the following, we will restrict the discussion to the corrected values m_c and f_c .

Figure 1 shows the probability distribution $P(e\phi)$ of the electrostatic energy $e\phi$ for an ionic charge of $q = e$, as calculated from histograms. The $P(e\phi)$ curves follow closely Gaussian distributions with mean and variance calculated from the ϕ data. This reflects the approximate validity of second-order perturbation theory in the ionic charge. However, the $P(e\phi)$ curves for Ewald summation with $N = 128$ and 256 , as well as GRF with $N = 256$ water molecules differ widely, both in the peak position and in the width. To illustrate the importance of the finite-size correction, we included in Figure 1 the Gaussian distributions corresponding to the corrected values m_c and f_c for mean and variance. The application of the finite-size corrections brings the three curves to very close agreement, yielding results that are approximately independent of system size and treatment of electrostatic interactions.

To further illustrate the importance of the finite-size correction, we calculated $\langle\phi\rangle$ from the pair correlations of the Ewald-summation simulation with $N = 256$ water molecules as

$$\langle\phi\rangle(R) = 4\pi\rho_{\text{H}_2\text{O}} \int_0^R dr r^2 \varphi(r) [q_{\text{O}}g_{\text{IO}}(r) + 2q_{\text{H}}g_{\text{IH}}(r)] . \quad (21)$$

$\rho_{\text{H}_2\text{O}}$ is the water density, q_{O} and q_{H} are the oxygen and hydrogen charge, and g_{IO} and g_{IH} are the ion-oxygen and ion-hydrogen pair correlation functions. Figure 2 shows the results for the charge-state $q = -e$ of the ion Me as a function of the integration cutoff R for the bare Coulomb potential $\varphi(r) = 1/r$ and φ_{GRF} with $r_c = L/2$. In both cases we included the finite-size correction as a constant. The integration of the $1/r$ interaction extended into the corners of the cube, using the correct weights. As a reference, the Ewald result is shown as a straight line. All three methods converge to within about 1 kJ mol $^{-1}$, which has to be compared with the estimated statistical error of 4 kJ mol $^{-1}$ of the data. The integrated $1/r$ interaction shows strong oscillations and only in the corners of the cube does it approach its final value. The GRF interaction on the other hand contains a large self term and within two oscillations reaches its limiting value.

This illustrates an important point regarding the correction of finite-size effects in the calculation of charge-related quantities. We achieve agreement between different methods of treating Coulomb interactions (Ewald summation, reaction field, bare Coulomb interaction) if we (i) normalize φ according to eq 14 and (ii) add a self term $\xi =$

$\lim_{\mathbf{r} \rightarrow 0} [\varphi(\mathbf{r}) - 1/r]$ to the energy. Further demonstrations of the validity of these finite-size corrections will be given in the discussion of the results for sodium and fluoride ions in SPC water.

Figure 3 shows m_c as a function of the charge. We observe two linear regimes with different characteristics for $q < 0$ and $q \geq 0$. Linear behavior of m_c on the whole range of q would reflect validity of the second-order perturbation theory. It would imply Gaussian statistics of ϕ and, correspondingly, that the coefficients in the Taylor expansion of order three and higher vanish. However, since we observe a transition in the linear behavior between charges of $-0.25e$ and 0 , the statistics are only approximately Gaussian. We note that from the ϕ data of 100 000 passes it proved impossible to extract reliable information about the Taylor coefficients (cumulants) of order three and higher. The second Taylor coefficient f_c can however be extracted accurately. Figure 4 shows f_c as a function of q/e . Included in Figure 4 as lines are the values of f_c estimated from the linear fits of m_c for $q < 0$ and $q \geq 0$.

We have fitted the m_c and f_c data by a model with two Gaussian regimes. Included in Figures 3 and 4 is a χ^2 fit of the whole set of derivative data (38 data points) to

$$\mu^{ex}(q) - \mu^{ex}(0) = (a_+q + b_+q^2)[1 + \tanh(c + dq)]/2 + (a_-q + b_-q^2)[1 - \tanh(c + dq)]/2, \quad (22)$$

where χ^2 is defined as in eq 5 with parameters a_+ , b_+ , a_- , b_- , c , and d . This model can nicely reproduce the data. We find a transition at $q = c/d \approx -0.2e$ between the two regimes of approximately Gaussian behavior with a quadratic q dependence. We ascribe this transition to differences in the structural organization of water molecules near negatively and positively charged ions. A possible explanation for the observed behavior is that for positive ions, the oxygen atom of water is pointing towards the LJ particle. The strongly repulsive forces of the r^{-12} interaction prevent large fluctuations of ϕ because of the restricted oxygen motions. The hydrogens are pointing away so that rearranging them has only a comparably small effect on ϕ . For negative ions, the structures with one of the hydrogens pointing towards the ion will dominate. Because of the symmetry between the water hydrogens and the finite life time of the hydration shell, transitions will occur which could explain the larger fluctuations in the negative charge range.

Similarly, a transition to a different Gaussian behavior for highly-charged positive ions was observed by Jayaram *et al.*² These authors studied the free energy of charging of a sodium ion in the charge range 0 to $3e$. When increasing the ion charge, a transition occurs to a more weakly decreasing quadratic free-energy regime at a charge of about $1.1e$. This transition has also been discussed by Figueirido *et al.*³⁴

We also find a nonvanishing potential at the methane site even at zero charge.⁵ In a dipolar solvent, $\langle \phi \rangle_{q=0}$ is zero because of charge-reversal symmetry. However, if higher multipole moments are present on the solvent molecule, this symmetry is not conserved. The asymmetry of the charge distribution on the water molecule gives rise to a positive potential for $q = 0$; this is primarily caused by the hydrogens penetrating the LJ sphere of the methane particle, since they do not have a protecting repulsive shell in the model used. As a consequence, there is a small charge region in which increasing the charge *costs* free energy. A positive potential at the center of an uncharged particle was also observed by Rick and Berne.³⁵

As a consequence of both the positive potential at zero charge and the larger potential fluctuations for negative ions, negative ions are more stably solvated compared to positive ions. Table III compiles the free energies of charging as calculated from fitted polynomials p_n of degree n to the derivative data m_c and f_c . Except for the simple Gaussian model p_2 , different fitting functions give consistent results for the free energies of charging. For ions with charge e and $-e$ we find $\Delta\mu^{ex} = -250$ and -431 kJ mol $^{-1}$. Interpreted within a Born model for the free energy,¹ *i.e.*,

$$\Delta\mu_{\text{Born}}^{ex} = -(1 - 1/\epsilon)q^2/2R, \quad (23)$$

we obtain Born radii $R_+ = 0.27$ nm and $R_- = 0.16$ nm. (A value of $\epsilon = 80$ is used for the dielectric constant, but this hardly affects the results). The difference between R_+ and R_- is somewhat smaller if we use the actual coefficients of the q^2 term in the free energy expansion, as obtained from eq 22, giving 0.23 and 0.16 nm for the Born radii of positive and negative ions. We emphasize the model character of the interaction potentials used in this study. A repulsive shell of the hydrogen atom might reduce the free energy difference between positive and negative ions. The favoring of negative ions however should persist.

The lower free energy of negative ions compared to positive ions of equal size agrees with the experimental observations. The hydration free-energy data compiled by Marcus³⁶ for alkali metal and halide ions show a power-law dependence with respect to the ion radius. Using these fitted curves, we find differences of 150 and 240 kJ mol $^{-1}$ for the solvation free energy between negative and positive ions of the size of potassium and sodium, respectively. The LJ particle Me studied here has a van der Waals radius between those of K^+ and Na^+ . The calculated free energy required to go from $-e$ to $+e$ is 180 kJ mol $^{-1}$, which is indeed bracketed by the experimental data.

The revised Born model by Latimer *et al.*³⁷ also yields lower free energies for negative ions. For alkali and halide ions, it uses effective Born radii $R = r_P + \Delta$, where r_P is the Pauling radius and Δ is 0.085 and 0.010 nm for cations and anions. This smaller effective-radius correction for anions in eq 23 results in considerably lower free energies of

negative ions compared to positive ions of equal size in agreement with our calculations. The difference of the effective Born-radius correction as defined by Latimer *et al.*³⁷ is 0.075 nm, which agrees with what we find for the Me ion.

The energetic differences in the hydration of positive and negative ions go along with differences in the structural organization of water molecules in the hydration shell. Figure 5 shows the ion-water pair correlation functions for different ionic charges. Going from $q = 0$ to positive charges does not change the qualitative properties of the ion-oxygen and ion-hydrogen correlation functions g_{IO} and g_{IH} . An increase of the ionic charge results in a higher first peak. However, going from charge $q = 0$ to negative charges affects strongly the structural organization of the first hydration shell. Already at $q = -0.5e$, g_{IH} shows the buildup of a second peak at about $r = 0.2$ nm distance. This peak reaches a value of almost 5 at $q = -e$, compared to g_{IH} essentially being zero in this distance region for charge $q = 0$. This strong interaction of the negatively charged ion with the hydrogens of water in turn affects the ion-oxygen correlation functions. Despite the negative charge of both the ion and oxygen site, g_{IO} has a first peak with a height of about 5 for $q = -e$ compared to only 3 for $q = e$. The strong charge repulsion between water oxygens and the ion with $q = -e$ is overcome by a large attraction caused by a water hydrogen pointing towards the ion and penetrating the ionic van der Waals shell without energetic penalty.

B. Free energy of charging of the ions Na^+ , K^+ , Ca^{2+} , F^- , Cl^- , and Br^-

Using the LJ parameters of Straatsma and Berendsen³² (see Table I), we computed solvation free energies of ions representing Na^+ , K^+ , Ca^{2+} , F^- , Cl^- , and Br^- . Again, we emphasize the model character of this study. Its purpose is not to provide accurate theoretical values for the free energies but rather to characterize the theory. We can expect to obtain accurate values only after considerable improvement of the currently rather crude descriptions of the interaction potentials used here and similarly in most other studies. Some of that work has indeed been guided by using free energies of hydration.^{38,39} However, controversies about certain technical aspects, primarily regarding the correct treatment of long-range interactions, need to be resolved to obtain conclusive results.^{40,41}

We extensively studied the solvation free energy of the sodium cation using the model described in section III. Monte Carlo simulations using $N = 128$ water molecules were carried out for charges 0, $0.5e$, and $1.0e$ to calculate the mean m_c and the fluctuation f_c of the electrostatic potential ϕ at the ion site. As in the previous calculations, 100 000 passes were used for averaging. The results are listed in Table IV. As for the uncharged methane, the potential at the uncharged sodium site is slightly positive. The decrease of m_c with increasing charge is stronger than linear and, correspondingly, the fluctuation f_c increases slightly with the charge. This indicates that a simple Gaussian model using an expansion around the uncharged particle is of limited utility.

We use the information about the derivatives to calculate the free energy of charging using polynomial fits. The results for the sodium ion using polynomials of degree 2, 4, and 6 are compiled in Table V. Also included in Table V are results obtained from TI, as described in section III. TI was performed using Ewald summation and $N = 8$, 16, 32, 64, 128, and 256 water molecules as well as using the GRF Coulomb interaction and $N = 32$, 64, and 128 water molecules. We observe excellent agreement of the free-energy data from polynomial fits and TI, except for the p_2 fit which cannot fully account for the increasing potential fluctuations with increasing charge. The TI data of charging from 0 to e and uncharging from e to 0 show variations of about 5 kJ mol⁻¹. Regarding the system-size dependence, Ewald summation gives accurate results even for as few as $N = 16$ water molecules. The GRF shows a more pronounced system-size dependence with the $N = 64$ data (cutoff $r_c = 0.62$ nm) being slightly too low. These results indicate that the free energy of charging is unexpectedly insensitive to the system size if the electrostatic interactions are treated appropriately. In particular, it is important to apply the correct finite-size corrections. For Ewald summation with $N = 16$, for instance, the finite-size correction accounts for about 60 percent of the free energy. Without the self terms the Ewald results for $N = 256$ and $N = 16$ differ by about 63 kJ mol⁻¹; with the self terms included the difference is only 5 kJ mol⁻¹.

Table VI lists the results of polynomial fits of the free energy to the derivative data for the other ions studied (K^+ , Ca^{2+} , F^- , Cl^- , and Br^-). Also included are results of TI calculations using Ewald summation and $N = 128$ water molecules. Except for the polynomial fit of degree 2, we obtain consistent results from the derivative data and TI. The p_2 results are always somewhat too negative but this is more apparent for the negative ions. The two TI data per ion typically bracket the p_4 and p_6 results for the free energy.

Interestingly, there is no simple trend for the free energy of charging of monovalent cations with the ion size (as measured by σ of the LJ interaction). The positive ions Na^+ and K^+ as well as the negative ions F^- , Cl^- , and Br^- show the expected decrease of $\Delta\mu^{ex}$ with increasing σ . However, only the negatively charged methane-like LJ particle Me^- fits into this ordering. The positively charged Me^+ has a less negative $\Delta\mu^{ex}$ than K^+ , even though the van der Waals diameter σ of K^+ is considerably larger. However, the LJ interaction of the K^+ ion is more shallow than that of Me^+ with the LJ ϵ values differing by a factor of about 150.

We also calculated the excess chemical potential of inserting uncharged LJ particles in SPC water of density $\rho = 33.33 \text{ nm}^{-3}$ at temperature $T = 298 \text{ K}$. This was done using test-particle insertion.^{15,42-50} 5000 SPC water configurations were used of a simulation run extending over 500 000 Monte Carlo passes. The simulation was performed using $N = 256$ water molecules and GRF Coulomb interaction with a cutoff of $r_c = 0.9 \text{ nm}$. We calculated $\langle \exp(-\beta u) \rangle$ using 100 test particles per configuration, where u is the interaction energy of a LJ test particle with the water molecules. For the LJ interaction, a spherical cutoff distance of $L/2 = 0.9865 \text{ nm}$ was used. A cutoff correction for the r^{-6} term was applied, assuming homogeneous water density beyond the cutoff. The excess chemical potential is calculated as

$$\mu^{ex} = -k_B T \ln \langle \exp(-\beta u) \rangle. \quad (24)$$

Results are listed in Table VII. We find positive values for μ^{ex} between 9 and 25 kJ mol^{-1} , favoring the gaseous state. Adding μ^{ex} to the free energy of charging, we obtain single-ion free energies of hydration.

Experimental data for single-ion free energies of hydration have been compiled by, for instance, Friedman and Krishnan,⁵¹ Conway,⁵² and most recently Marcus.³⁶ The first two references report values for the standard molar Gibbs free energy ΔG^0 , *i.e.*, for a hypothetical transfer from a 1 atm gas state to a 1 mol/l solution. Marcus lists values for ΔG^* which is the Gibbs free energy of bringing an ion from an empty box into solution. The theoretical calculations determine the excess free energy of hydration, *i.e.*, the transfer from an ideal gas of given density to solution of equivalent solute density. This process corresponds to that used by Marcus, so that ΔG^* is the experimental equivalent of the theoretical free energy that we have referred to as μ^{ex} disregarding volume contributions. Because Marcus used ΔG^* for the experimental free energies of hydration we will retain that notation here for those quantities. To convert from ΔG^0 to ΔG^* , requires adjustment for the differences in standard states: we add to ΔG^0 the free energy of an ideal gas going from a pressure p_0 corresponding to a density of 1 mol/l to a pressure $p_1 = 1 \text{ atm}$, which is $k_B T \ln(p_1/p_0)$, *i.e.*, $\Delta G^* = \Delta G^0 - 7.92 \text{ kJ mol}^{-1}$.⁵³ Another correction accounts for differing values for the reference ion H^+ . We take the most recent value by Marcus³⁶ $\Delta G^*[\text{H}^+] = -1050 \pm 6 \text{ kJ mol}^{-1}$ and adjust the other values $[-1098 \text{ (ref 51)} \text{ and } -1074 \pm 17 \text{ kJ mol}^{-1} \text{ (ref 52)}]$ accordingly.

Results for the calculated free energy of ionic hydration $\mu^{ex} = \mu^{ex}(q = 0) + \Delta\mu^{ex}(0 \rightarrow q)$ and the experimental values ΔG^* are compiled in Table VIII. For the calculated values we use those obtained from a fit of a sixth-order polynomial p_6 to the derivative data, as listed in Table VI. The experimental data were adjusted as described above. The experimental data for cations show little variation between the three sources. However, the anion data vary by as much as 70 kJ mol^{-1} , with the Conway data⁵² bracketed by the those of refs 36 and 51, but generally closer to the data of Marcus.³⁶

The calculated free energy data for cations do not show a clear trend. The results for Na^+ and K^+ are too low and too high by about 10 percent, respectively. The hydration free energy of Ca^{2+} is too high by about 15 percent. The anions on the other hand show a clear tendency with the magnitudes of the calculated free energies generally being too large. The relative errors are 26, 10, and 15 percent for F^- , Cl^- , and Br^- , respectively, compared to the data of Marcus. These significantly too negative values of the hydration free energy of anions might be a consequence of the unprotected hydrogen atoms in the water-ion interaction model used. The positively charged hydrogen atom can penetrate the LJ shell of the ions without a direct energetic penalty. The interaction with the negative point charge at the center of the ion strongly binds the water molecule, resulting in a large enthalpic contribution to the free energy of hydration. But also effects of non-additive interactions might play a considerable role.⁵⁴

Also included in Table VIII are computer simulation results by Straatsma and Berendsen.³² These authors used thermodynamic integration in conjunction with isothermal-isobaric molecular dynamics simulations to compute hydration free energies of ions. The interaction potentials used here are identical with those of Straatsma and Berendsen, except for the treatment of the electrostatic interactions. We used Ewald summation; whereas Straatsma and Berendsen used a spherical cutoff and a Born-type correction for finite-size effects. These authors (and others³⁹) argue that the application of a Born-type correction is rather crude, approximating the solvent molecules beyond the cutoff by a dielectric continuum. Nevertheless, in the absence of a better alternative it has been widely adopted. Migliore *et al.*⁵⁵ calculated the free energy of ionic hydration based on a perturbation formula from Monte Carlo simulations using MCY water and *ab initio* ion-water potentials. These authors also used a spherical cutoff. Table VIII includes the results of Migliore *et al.*, who did not apply a finite-size correction.

Qualitatively, our free-energy data agree with those of Straatsma and Berendsen³² and Migliore *et al.*⁵⁵ We observe the same ordering of the free energies with respect to ion size. The quantitative agreement is however poor. Our values for the cations Na^+ and K^+ are closer to the experimental data of Marcus. The cation free energies of Straatsma and Berendsen (with Born correction) are consistently more negative than those of our calculations. On the other hand, our anion free energies are significantly more negative than those of Straatsma and Berendsen as well as of Migliore *et al.* The results of Straatsma and Berendsen for Cl^- and Br^- are somewhat closer to the experimental data of Marcus when the Born correction is included. Without the correction they are significantly too high. The most

pronounced discrepancies between the anion data of Straatsma and Berendsen³² and ours are those of the fluoride ion, with our μ^{ex} values being lower by 83 kJ mol⁻¹. This is somewhat surprising since Straatsma and Berendsen used the same parameters for the water-water and water-ion interactions. The difference can be a consequence of using different ensembles (NVT versus quasi-NPT); or, more likely, it is caused by the different treatment of the electrostatic interactions (Ewald versus spherical cutoff).

The fluoride ion also shows the largest relative deviations from the experimental results. To further investigate these discrepancies, we have studied the energetics of clusters of different size formed by a single fluoride ion and water. We have performed Monte Carlo simulations using one F⁻ ion that nucleates $N = 4, 8, 12, 16, 32, 64, 128$, and 256 water molecules at 298 K, as described in section III. We calculated the interaction energy u_s of the fluoride ion with the SPC water molecules over 50 000 passes. Figure 6 shows the differences $\Delta u_s = u_s - u_{s,EW}$ with respect to the bulk simulation using $N = 128$ water molecules and Ewald summation as a function of $N^{-1/3}$. Δu_s can be fitted to a third-order polynomial in $N^{-1/3}$ over the whole range of system sizes. Extrapolation to $N \rightarrow \infty$ yields a limit for Δu_s close to zero. (However, the nontrivial dependence on $N^{-1/3}$ limits the accuracy of the extrapolation.) The result obtained from Ewald summation, $u_{s,EW} = -1077 \pm 4$ kJ mol⁻¹, also agrees with the value $u_s = -1075$ kJ mol⁻¹ obtained from integrating the pair correlation functions of the bulk simulation using $\varphi(r) = 1/r$ in eq 21, adding the LJ contributions, and applying the finite-size correction $-e^2 \xi_{1/r}$. The integration shows that the LJ contributions are strongly repulsive (≈ 90 kJ mol⁻¹) but compensated by large electrostatic interactions.

The value for the solvation energy reported by Straatsma and Berendsen, $u_s = -823$ kJ mol⁻¹, is however considerably smaller. The observed differences in u_s of about 150 kJ mol⁻¹ agree in magnitude and sign with those of the free energies (83 kJ mol⁻¹). If we truncate the integration of $1/r$ weighted with the pair correlation functions obtained from Ewald summation at $R = 0.9$ nm (which is the cutoff Straatsma and Berendsen used) and do not apply a finite-size correction, we obtain a value of -867 kJ mol⁻¹ in much closer agreement with Straatsma and Berendsen's. This indeed indicates that the treatment of the electrostatic interactions (Ewald summation versus spherical cutoff) is the major source of the discrepancy.

Also included in Figure 6 are the results for the mean and the variance of the electrostatic potential at the ion site. Figure 6 shows differences with respect to the bulk value. The differences of the mean values $\Delta \langle \phi \rangle$ closely follow the solvation-energy differences Δu_s and can also be fitted to a third-order polynomial in $N^{-1/3}$. The differences of the fluctuation $\Delta \langle \Delta \phi^2 \rangle$ depend linearly on $N^{-1/3}$ for N between 8 and 256. Both fitted curves extrapolate to approximately 0, indicating that the calculated bulk values are the correct limits for $N \rightarrow \infty$.

From the cluster-size dependence of the solvation energy and the mean and variance of the electrostatic potential, as well as the results for Me and Na⁺, we conclude that the use of periodic boundary conditions in conjunction with Ewald-summation (or reaction-field) electrostatics closely approximates the correct bulk behavior of the system; however, to get correct energetics it is important to include the self-interactions in the Coulomb energy.

V. CONCLUSIONS

We have shown that free energies can be accurately calculated from equilibrium simulations by extracting derivative information with respect to a coupling parameter. We have studied the free energy of charging ions in water, which accounts for most of the free energy of ionic solvation for typical ion sizes. The choice of the ionic charge as coupling parameter results in free-energy expressions involving cumulants of the electrostatic potential ϕ at the charge sites. We find that the statistics of ϕ are approximately Gaussian. This means that only the first and second moment of the distribution can be calculated accurately, with higher moments dominated by the poorly sampled tails. Correspondingly, only information about the first and second derivative of the free energy can be calculated accurately for any given charge state. The information for different charge states (*e.g.*, uncharged and fully charged) can then be combined using interpolation or polynomial fitting.

We have studied a methane-like Lennard-Jones particle in SPC water. We observe two almost Gaussian regimes separated by $q = 0$ with different characteristics. Negative ions are more stably solvated compared to positive ions of equal size, in agreement with the experimental data.³⁷ The system shows further asymmetry, since the average electrostatic potential at the position of the uncharged particle is positive. This means that increasing the ion charge first costs energy. We relate these asymmetries of the energetics (lower free energy of negative ions, positive potential) to the structural asymmetry of the water molecule. The hydrogen atoms can penetrate the ionic van der Waals shell, whereas the oxygen atom is better protected. For the uncharged particle, this results in a net positive potential; and the point charge at the center of negative ions exerts strong electrostatic interactions with the tightly bound hydrogen of water.

However, particularly for small anions this effect might be exaggerated by the interaction potentials used. This potential model does not give a protective van der Waals sphere to the charge on the hydrogen atom. In principle,

this is a fundamental difficulty, but in computer simulations, the heights of energetic barriers usually exclude the singularity. The development of interaction potentials for anion-water interactions nevertheless has to account for these problems. The strong interactions with the hydrogens “pull” the water closer and the first maxima of the ion-oxygen pair correlation function is already in the strongly repulsive region, reducing the effective ion radius.

We have also studied the charging of sodium, potassium, calcium, fluoride, chloride, and bromide ions. The agreement with the available experimental data for solvation free energies is only qualitative, reproducing the trends with ionic size. The quantitative data are not in satisfactory agreement with the experimental results, even conceding quite substantial discrepancies between different compilations of the experimental data for certain ions. We observe typical errors of about 10 to 15 percent for the free energies of ionic solvation compared to the experimental data of Marcus.³⁶ This clearly indicates the further need to develop quantitatively reliable descriptions of ion-water interactions.

However, to allow for valid comparisons of data obtained from computer simulations with experimental results, it is crucial to eliminate systematic errors in the simulation methods. An important part of this study was devoted to analyzing the effect of finite system sizes on the free energy of charging. We could clearly establish that Ewald summation (and, similarly, the generalized reaction-field method) accounts for finite-size effects by adding a term that corrects for self-interactions. We showed that even for systems with only $N = 16$ water molecules it is possible to obtain accurate estimates of the solvation free energy of the sodium ion. For typical system sizes of a few hundred water molecules, these finite-size corrections are substantial in magnitude. Neglecting them yields results of little quantitative validity.

ACKNOWLEDGMENTS

G. H. wishes to thank M. Neumann and D. M. Soumpasis for many stimulating discussions. This work was funded by the Department of Energy (U.S.).

- ¹ Born, M. *Z. Phys.* **1920**, *1*, 45.
- ² Jayaram, B.; Fine, R.; Sharp, K.; Honig, B. *J. Phys. Chem.* **1989**, *93*, 4320.
- ³ Levy, R. M.; Belhadj, M.; Kitchen, D. B. *J. Chem. Phys.* **1991**, *95*, 3627.
- ⁴ Smith, P. E.; van Gunsteren, W. F. *J. Chem. Phys.* **1994**, *100*, 577.
- ⁵ Pratt, L. R.; Hummer, G.; García, A. E. *Biophys. Chem.* **1994**, *51*, 147.
- ⁶ Tawa, G. J.; Pratt, L. R. In Cramer, C. J.; Truhlar, D. G., Eds. *Structure and Reactivity in Aqueous Solution: Characterization of Chemical and Biological Systems. ACS Symposium Series*; ACS: Washington DC, 1994, Vol. 568, p. 60.
- ⁷ Tawa, G. J.; Pratt, L. R. *J. Am. Chem. Soc.* **1995**, *117*, 1625.
- ⁸ Honig, B.; Sharp, K.; Yang, A.-S. *J. Phys. Chem.* **1993**, *97*, 1101.
- ⁹ Warshel, A.; Chu, Z. T. In Cramer, C. J.; Truhlar, D. G., Eds. *Structure and Reactivity in Aqueous Solution: Characterization of Chemical and Biological Systems. ACS Symposium Series*; ACS: Washington DC, 1994, Vol. 568, p. 71.
- ¹⁰ Marcus, Y. *Biophys. Chem.* **1994**, *51*, 111.
- ¹¹ Neumann, M. *Mol. Phys.* **1983**, *50*, 841.
- ¹² Frenkel, D. In Ciccotti, G.; Hoover, W. G., Eds. *Molecular Dynamics Simulations of Statistical Mechanical Systems. Proceedings of the Enrico Fermi Summer School, Varenna, 1985*; North-Holland: Amsterdam, 1986, pp. 151–188.
- ¹³ Allen, M. P.; Tildesley, D. J. *Computer Simulation of Liquids*; Clarendon Press: Oxford, UK, 1987.
- ¹⁴ Levesque, D.; Weis, J. J. In Binder, K., Ed. *The Monte Carlo Method in Condensed Matter Physics*; Springer: Berlin, 1992, pp. 121–204.
- ¹⁵ Widom, B. *J. Phys. Chem.* **1982**, *86*, 869.
- ¹⁶ Kubo, R. *J. Phys. Soc. Jpn.* **1962**, *17*, 1100.
- ¹⁷ Hummer, G.; Soumpasis, D. M. *J. Chem. Phys.* **1993**, *98*, 581.
- ¹⁸ Ewald, P. P. *Ann. Phys.* **1921**, *64*, 253.
- ¹⁹ de Leeuw, S. W.; Perram, J. W.; Smith, E. R. *Proc. R. Soc. Lond. A* **1980**, *373*, 27.
- ²⁰ de Leeuw, S. W.; Perram, J. W.; Smith, E. R. *Ann. Rev. Phys. Chem.* **1986**, *37*, 245.
- ²¹ Cichocki, B.; Felderhof, B. U.; Hinsen, K. *Phys. Rev. A* **1989**, *39*, 5350.
- ²² Nijboer, B. R. A.; Ruijgrok, T. W. *J. Stat. Phys.* **1988**, *53*, 361.
- ²³ Placzek, G.; Nijboer, B. R. A.; van Hove, L. *Phys. Rev.* **1951**, *82*, 392.
- ²⁴ Hummer, G.; Soumpasis, D. M.; Neumann, M. *Mol. Phys.* **1992**, *77*, 769.
- ²⁵ Hummer, G.; Soumpasis, D. M. *Phys. Rev. E* **1994**, *49*, 591.

²⁶ Hummer, G.; Soumpasis, D. M.; Neumann, M. *J. Phys.: Condens. Matt.* **1994**, *23A*, A141.

²⁷ Sloth, P.; Sørensen, T. S. *Chem. Phys. Lett.* **1990**, *173*, 51.

²⁸ Refs 22 and 29 present rather lengthy calculations of the numerical value of $\xi_{1/r}$. We note that the integral of $1/r$ over a cubic volume can easily be obtained by summing the results of partial integration in each of the 3 dimensions,

$$\begin{aligned} -L\xi_{1/r} &= \int_{-1/2}^{1/2} dx \int_{-1/2}^{1/2} dy \int_{-1/2}^{1/2} dz (x^2 + y^2 + z^2)^{-1/2} \\ &= \frac{3}{2} \int_{-1/2}^{1/2} dx \int_{-1/2}^{1/2} dy (x^2 + y^2 + 1/4)^{-1/2} \\ &= \frac{3}{2} \int_{-1/2}^{1/2} dx \left\{ \ln \left[(4x^2 + 2)^{1/2} + 1 \right] - \ln \left[(4x^2 + 2)^{1/2} - 1 \right] \right\} \\ &= 3 \ln (3^{1/2} + 2) - \pi/2. \end{aligned}$$

²⁹ Sørensen, T. S. *J. Chem. Soc. Faraday Trans.* **1991**, *87*, 479.

³⁰ Metropolis, N.; Rosenbluth, A. W.; Rosenbluth, M. N.; Teller, A. H.; Teller, E. *J. Chem. Phys.* **1953**, *21*, 1087.

³¹ Berendsen, H. J. C.; Postma, J. P. M.; van Gunsteren, W. F.; Hermans, J. In Pullman, B., Ed. *Intermolecular Forces: Proceedings of the 14th Jerusalem Symposium on Quantum Chemistry and Biochemistry*; Reidel: Dordrecht, Holland, 1981, pp. 331–342.

³² Straatsma, T. P.; Berendsen, H. J. C. *J. Chem. Phys.* **1988**, *89*, 5876.

³³ Jorgensen, W. L.; Madura, J. D.; Swenson, C. J. *J. Am. Chem. Soc.* **1984**, *106*, 6638.

³⁴ Figueirido, F.; Del Buono, G. S.; Levy, R. M. *Biophys. Chem.* **1994**, *51*, 235.

³⁵ Rick, S. W.; Berne, B. J. *J. Am. Chem. Soc.* **1994**, *116*, 3949.

³⁶ Marcus, Y. *J. Chem. Soc. Faraday Trans.* **1991**, *87*, 2995.

³⁷ Latimer, W. M.; Pitzer, K. S.; Slansky, C. M. *J. Chem. Phys.* **1939**, *7*, 108.

³⁸ Åqvist, J. *J. Phys. Chem.* **1990**, *94*, 8021.

³⁹ Marrone, T. J.; Merz Jr., K. M. *J. Phys. Chem.* **1993**, *97*, 6524.

⁴⁰ Åqvist, J. *J. Phys. Chem.* **1994**, *98*, 8253.

⁴¹ Marrone, T. J.; Merz Jr., K. M. *J. Phys. Chem.* **1994**, *98*, 8256.

⁴² Pohorille, A.; Pratt, L. R. *J. Am. Chem. Soc.* **1990**, *112*, 5066.

⁴³ Pratt, L. R.; Pohorille, A. *Proc. Natl. Acad. Sci. USA* **1992**, *89*, 2995.

⁴⁴ Pratt, L. R.; Pohorille, A. In Palma, M. U.; Palma-Vittorelli, M. B.; Parak, F., Eds. *Proceedings of the EBSA (Association of the European Biophysical Societies) 1992 International Workshop on Water-Biomolecule Interactions*; Societa' Italiana de Fisica: Bologna, 1993, pp. 261–268.

⁴⁵ Guillot, B.; Guissani, Y.; Bratos, S. *J. Chem. Phys.* **1991**, *95*, 3643.

⁴⁶ Guillot, B.; Guissani, Y. *J. Chem. Phys.* **1993**, *99*, 8075.

⁴⁷ Guillot, B.; Guissani, Y. *Mol. Phys.* **1993**, *79*, 53.

⁴⁸ Madan, B.; Lee, B. *Biophys. Chem.* **1994**, *51*, 279.

⁴⁹ Forsman, J.; Jönsson, B. *J. Chem. Phys.* **1994**, *101*, 5116.

⁵⁰ Beutler, T. C.; Béguelin, D. R.; van Gunsteren, W. F. *J. Chem. Phys.* **1995**, *102*, 3787.

⁵¹ Friedman, H. L.; Krishnan, C. V. In Franks, F., Ed. *Water: A Comprehensive Treatise*; Plenum: New York, 1973, Vol. 3, pp. 1–118.

⁵² Conway, B. E. *J. Solution Chem.* **1978**, *7*, 721.

⁵³ Interestingly, Marcus^{10,36} finds the correction to be of opposite sign. Straatsma and Berendsen³² however determine a correction identical to ours. Assuming the tabulated values of Marcus to be correct, this does however not affect the following discussion.

⁵⁴ Xantheas, S. S.; Dunning and Jr., T. H. *J. Phys. Chem.* **1992**, *96*, 7505.

⁵⁵ Migliore, M.; Corongiu, G.; Clementi, E.; Lie, G. C. *J. Chem. Phys.* **1988**, *88*, 7766.

FIG. 1. Probability distributions $P(e\phi)$ of the electrostatic energy $e\phi$ at the site of a methane-like ion Me with charge $q = e$ from Ewald summation with $N = 256$ (\diamond , —), $N = 128$ (\square , $-\cdot-$), and GRF with $N = 256$ water molecules (+, $--$), respectively. The lines are Gaussian distributions. Also shown are Gaussian distributions corrected for finite-size effects, which are peaked near $e\phi = -550$ kJ mol⁻¹; they agree closely in position and variance.

FIG. 2. The average electrostatic potential ϕ at the site of the negatively charged ion Me ($q = -e$) calculated from the pair correlations of a Monte Carlo simulation using Ewald summation and $N = 256$ water molecules. The results of the integration using the GRF interaction with cutoff $r_c = L/2$ and the bare Coulomb interaction $1/r$ are shown with long- and short-dashed lines, respectively. Finite-size corrections are added as constants. The Ewald-summation result is shown as a reference with a solid line.

FIG. 3. The average electrostatic potential m_c at the position of the methane-like Lennard-Jones particle Me as a function of its charge q . m_c contains corrections for the finite system size. Results are shown from Monte Carlo simulations using Ewald summation with $N = 256$ (+) and $N = 128$ (\times) as well as GRF calculations with $N = 256$ water molecules (\square). Statistical errors are smaller than the size of the symbols. Also included are linear fits to the data with $q < 0$ and $q \geq 0$ (solid lines). The fit to the tanh-weighted model of two Gaussian distributions (eq 22) is shown with a dashed line.

FIG. 4. The fluctuation of the electrostatic potential f_c at the position of a methane-like Lennard-Jones particle as a function of its charge q . f_c contains corrections for the finite system size. Error bars indicate one estimated standard deviation of the data. For further details see Figure 3.

FIG. 5. The pair correlation functions g_{IO} (top panel) and g_{IH} (bottom panel) of the Me ion with water oxygen and hydrogen. The $g(r)$ curves are shifted vertically according to the ionic charge by q/e , *i.e.*, by 1 for $q = e$, 0.5 for $q = 0.5e$ etc. The $g(r)$ curves of Ewald summation and GRF simulations with $N = 256$ water molecules are shown with solid and dashed lines, respectively.

FIG. 6. The energetics of clusters of a fluoride ion and SPC water. Results are shown for the interaction energy u_s of the fluoride ion with the water (\diamond), as well as the mean $\langle \phi \rangle$ (+) and variance $\langle \Delta\phi^2 \rangle$ (\square) of the electrostatic potential at the ion position. The figure shows differences of these quantities with respect to the bulk values calculated from Monte Carlo simulation of an $N = 128$ water-molecule system using Ewald summation: $\Delta u_s = u_s - u_{s,\text{EW}}$, $\Delta \langle \phi \rangle = \langle \phi \rangle - \langle \phi \rangle_{\text{EW}}$, and $\Delta \langle \Delta\phi^2 \rangle = \langle \Delta\phi^2 \rangle - \langle \Delta\phi^2 \rangle_{\text{EW}}$. The lines are fitted curves as explained in the text. Error bars indicate one standard deviation estimated from block averages. The standard deviations of the bulk and cluster data were added.

TABLE I. Lennard-Jones parameters of the ion-water interactions.

Ion	$\epsilon/(\text{kJ mol}^{-1})$	σ/nm
Na ⁺	0.200546	0.285000
K ⁺	0.006070	0.452000
Ca ²⁺	0.637972	0.317000
F ⁻	0.553830	0.305000
Cl ⁻	0.537866	0.375000
Br ⁻	0.494464	0.383000
Me	0.893228	0.344778

TABLE II. Results for the mean and the fluctuation of the potential ϕ (with and without finite-size corrections) at the position of a methane-like Lennard-Jones particle Me carrying a charge q . ‘‘Coulomb’’ refers to the treatment of the electrostatic interactions (Ewald or GRF). N is the number of water molecules. The mean and the fluctuation are listed as $m = e\langle\phi\rangle$ and $f = \beta e^2 \langle(\phi - \langle\phi\rangle)^2\rangle$, both in units of kJ mol^{-1} . The corrected values are $m_c = m + qe\xi$ and $f_c = f - e^2\xi$. The statistical errors of m and f are estimated from block averages as approximately 4.0 and 30 kJ mol^{-1} .

N	Coulomb	q/e	m	f	m_c	f_c
256	EW	-1.00	670.3	604	869.9	804
128	EW	-1.00	618.1	664	869.2	915
256	GRF	-1.00	520.5	493	869.1	842
128	EW	-0.75	465.3	730	653.6	981
256	EW	-0.50	324.0	713	423.7	913
128	EW	-0.50	292.2	698	417.8	950
256	GRF	-0.50	242.2	568	416.5	917
128	EW	-0.25	141.3	529	204.0	780
256	EW	0.00	38.0	367	38.0	567
128	EW	0.00	37.3	341	37.3	592
256	GRF	0.00	34.9	239	34.9	587
128	EW	0.25	-40.7	313	-103.5	564
256	EW	0.50	-143.1	374	-242.9	573
128	EW	0.50	-118.1	332	-243.6	583
256	GRF	0.50	-74.4	232	-248.7	581
128	EW	0.75	-205.9	354	-394.2	605
256	EW	1.00	-348.8	450	-548.3	650
128	EW	1.00	-298.9	389	-550.0	640
256	GRF	1.00	-202.2	296	-550.9	645

TABLE III. Free energy (in kJ mol^{-1}) of charging the methane-like Lennard-Jones particle Me from 0 to $\pm e$. The free energy was calculated from fitting to polynomials p_n of degree n and a tanh-weighted model of two Gaussian regimes (eq 22).

Function	$\Delta\mu^{ex}(0 \rightarrow e)$	$\Delta\mu^{ex}(0 \rightarrow -e)$
p_2	-246	-454
p_4	-253	-431
p_6	-250	-431
p_8	-250	-431
p_{10}	-250	-431
tanh	-250	-430

TABLE IV. Results for the mean m_c and fluctuation f_c of the potential (with finite-size corrections included) at the position of sodium, potassium, calcium, fluoride, chloride, and bromide ions at different charge-states q . The data were calculated from Monte Carlo simulations using $N = 128$ water molecules and Ewald summation over 100 000 passes. The mean and the fluctuation are listed as $m_c = e(\langle \phi \rangle + q\xi)$ and $f_c = \beta e^2 \langle (\phi - \langle \phi \rangle)^2 \rangle - e^2 \xi$, both in units of kJ mol^{-1} . The statistical errors of m_c and f_c are estimated from block averages to be approximately 4.0 and 30 kJ mol^{-1} .

Ion	q/e	m_c	f_c
Na	0.00	39.0	891
Na	0.50	-395.6	956
Na	1.00	-885.1	970
K	0.00	38.6	682
K	0.50	-282.1	690
K	1.00	-662.6	772
Ca	0.00	41.0	662
Ca	1.00	-653.6	789
Ca	2.00	-1367.6	667
F	0.00	35.7	718
F	-0.50	587.6	1381
F	-1.00	1167.3	961
Cl	0.00	36.2	550
Cl	-0.50	378.2	819
Cl	-1.00	794.1	773
Br	0.00	37.3	545
Br	-0.50	369.2	758
Br	-1.00	772.7	773

TABLE V. Results for the free energy μ^{ex} of charging the sodium cation from $q = 0$ to e in SPC water in units of kJ mol^{-1} . μ^{ex} includes the finite-size corrections which are listed as μ_{self}^{ex} . The free energies were calculated from polynomial fits to the derivative data of Table IV (polynomials p_n of degree n). Also included are results of thermodynamic integration (TI). Linear charging paths from 0 to e and from e to 0 are denoted by upward (\uparrow) and downward (\downarrow) arrows, respectively. Ewald (EW) and generalized reaction-field (GRF) interactions were used for the charges.

Method	Coulomb	N	μ_{self}^{ex}	μ^{ex}
p_2	EW	128	-126	-415
p_4	EW	128	-126	-407
p_6	EW	128	-126	-407
TI \uparrow	EW	256	-100	-404
TI \downarrow	EW	256	-100	-406
TI \uparrow	EW	128	-126	-402
TI \downarrow	EW	128	-126	-407
TI \uparrow	EW	64	-158	-407
TI \downarrow	EW	64	-158	-406
TI \uparrow	EW	32	-198	-403
TI \downarrow	EW	32	-198	-407
TI \uparrow	EW	16	-247	-409
TI \downarrow	EW	16	-247	-411
TI \uparrow	EW	8	-305	-419
TI \downarrow	EW	8	-305	-425
TI \uparrow	GRF	128	-219	-401
TI \downarrow	GRF	128	-219	-406
TI \uparrow	GRF	64	-276	-408
TI \downarrow	GRF	64	-276	-411
TI \uparrow	GRF	32	-346	-419
TI \downarrow	GRF	32	-346	-424

TABLE VI. Results for the free energy μ^{ex} of charging the potassium, calcium, fluoride, chloride, and bromide ions from $q = 0$ to $\pm e, 2e$ in SPC water in units of kJ mol^{-1} . μ^{ex} includes finite-size corrections. Details as in Table V.

Ion	p_2	p_4	p_6	TI \uparrow	TI \downarrow
K^+	-297	-293	-295	-291	-294
Ca^{2+}	-1317	-1315	-1316	-1311	-1327
F^-	-594	-590	-590	-590	-594
Cl^-	-401	-392	-392	-389	-394
Br^-	-393	-382	-382	-379	-382

TABLE VII. Results for the excess chemical potential μ^{ex} (in kJ mol^{-1}) of transferring an uncharged LJ particle from ideal gas into SPC water. The LJ parameters are those of Table I. Errors are estimated from block averages.

LJ-Particle	μ^{ex}
Na	9.2(1)
K	23.7(5)
Ca	10.2(3)
F	9.7(2)
Cl	21(3)
Br	24(3)
Me	10.2(9)

TABLE VIII. Results for the calculated free energy of ionic hydration (in kJ mol^{-1}) compared with experimental data. The experimental data were adjusted to give $\Delta G^* = -1050 \text{ kJ mol}^{-1}$ for H^+ , as used by Marcus.³⁶ Also included are computer simulation results by Straatsma and Berendsen³² and Migliore *et al.*⁵⁵

Ion	μ^{ex}	ΔG^* ^a	ΔG^* ^b	ΔG^* ^c	μ^{ex} ^d	μ^{ex} ^e	μ^{ex} ^f
Na^+	-398	-365	-371	-372	-508	-431	-459
K^+	-271	-295	-298	-298	-425	-349	-321
Ca^{2+}	-1306	-1505	-1553	—	-1623	-1394	—
F^-	-580	-465	-394	-441	-497	-421	-418
Cl^-	-371	-340	-277	-324	-315	-239	-237
Br^-	-358	-315	-263	-310	-304	-228	—

^aExperimental data of Marcus.³⁶

^bExperimental data of Friedman and Krishnan.⁵¹

^cExperimental data of Conway.⁵²

^dComputer simulation data of Straatsma and Berendsen calculated using molecular dynamics of $N = 216$ water molecules.³² The results contain a Born-type correction applied by the authors to their raw data.

^eComputer simulation data of Straatsma and Berendsen without Born correction.³²

^fComputer simulation data of Migliore *et al.* calculated using molecular dynamics of $N = 342$ water molecules.⁵⁵

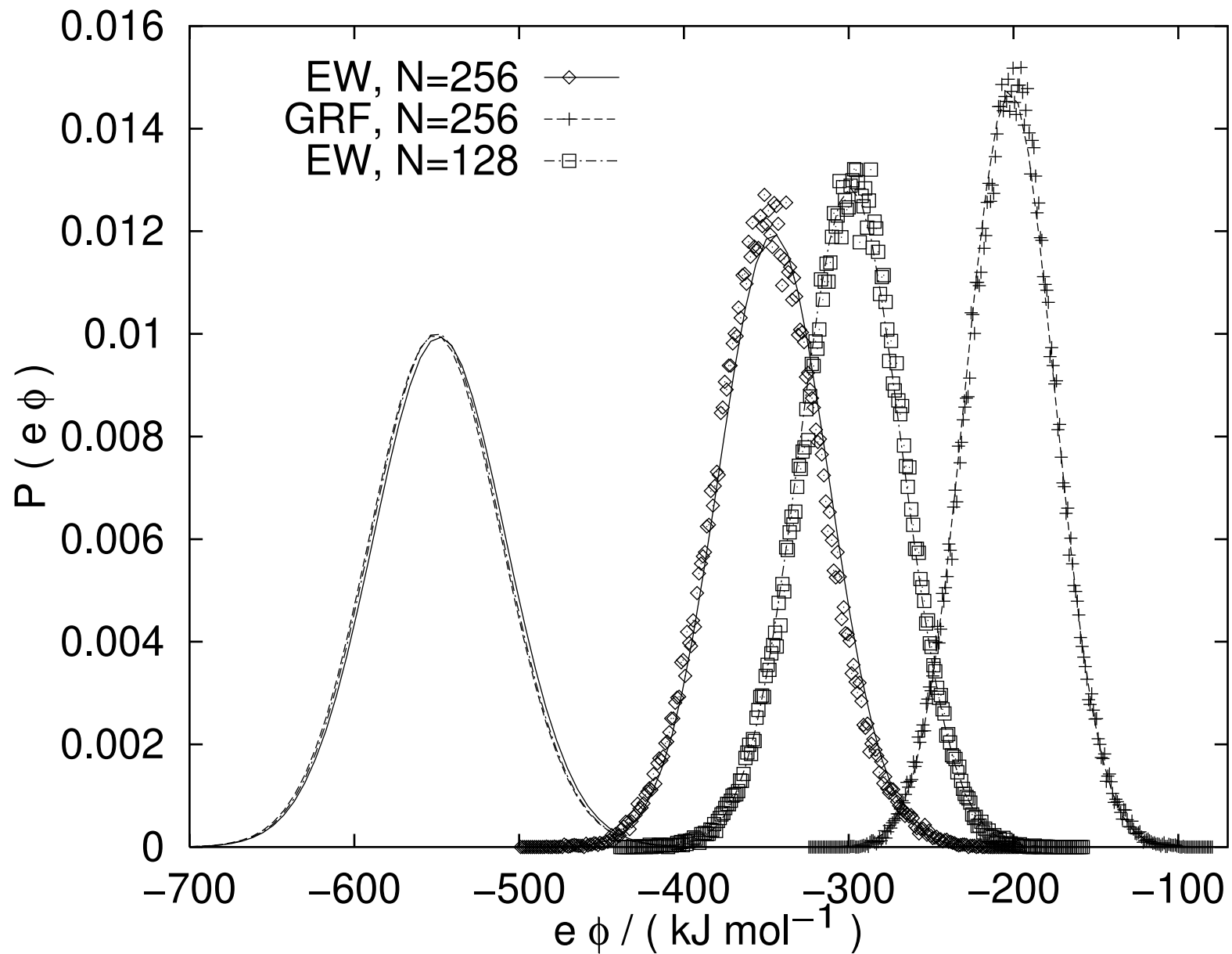


Fig. 1 (Hummer, Pratt, and Garcia)

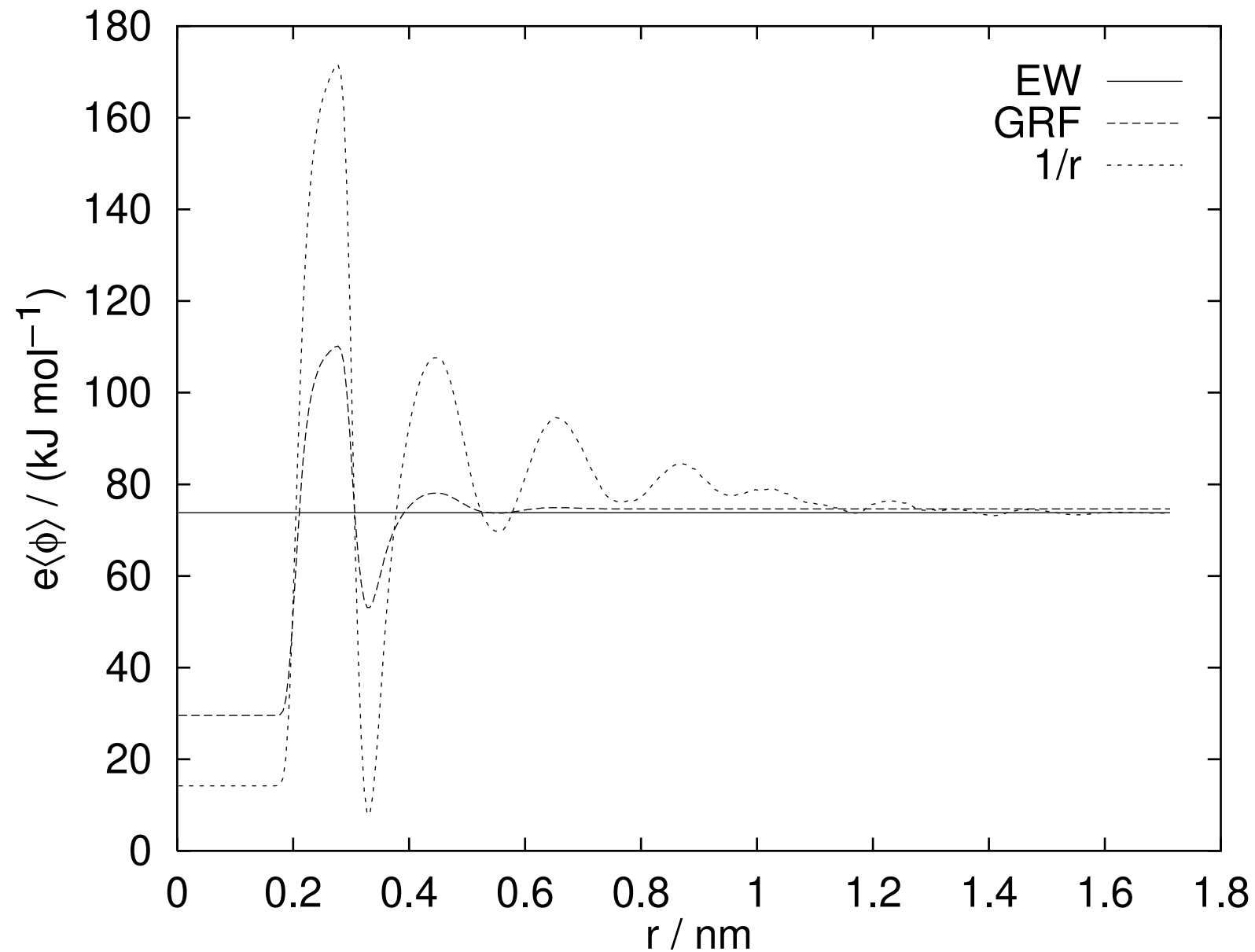


Fig. 2 (Hummer, Pratt, and Garcia)

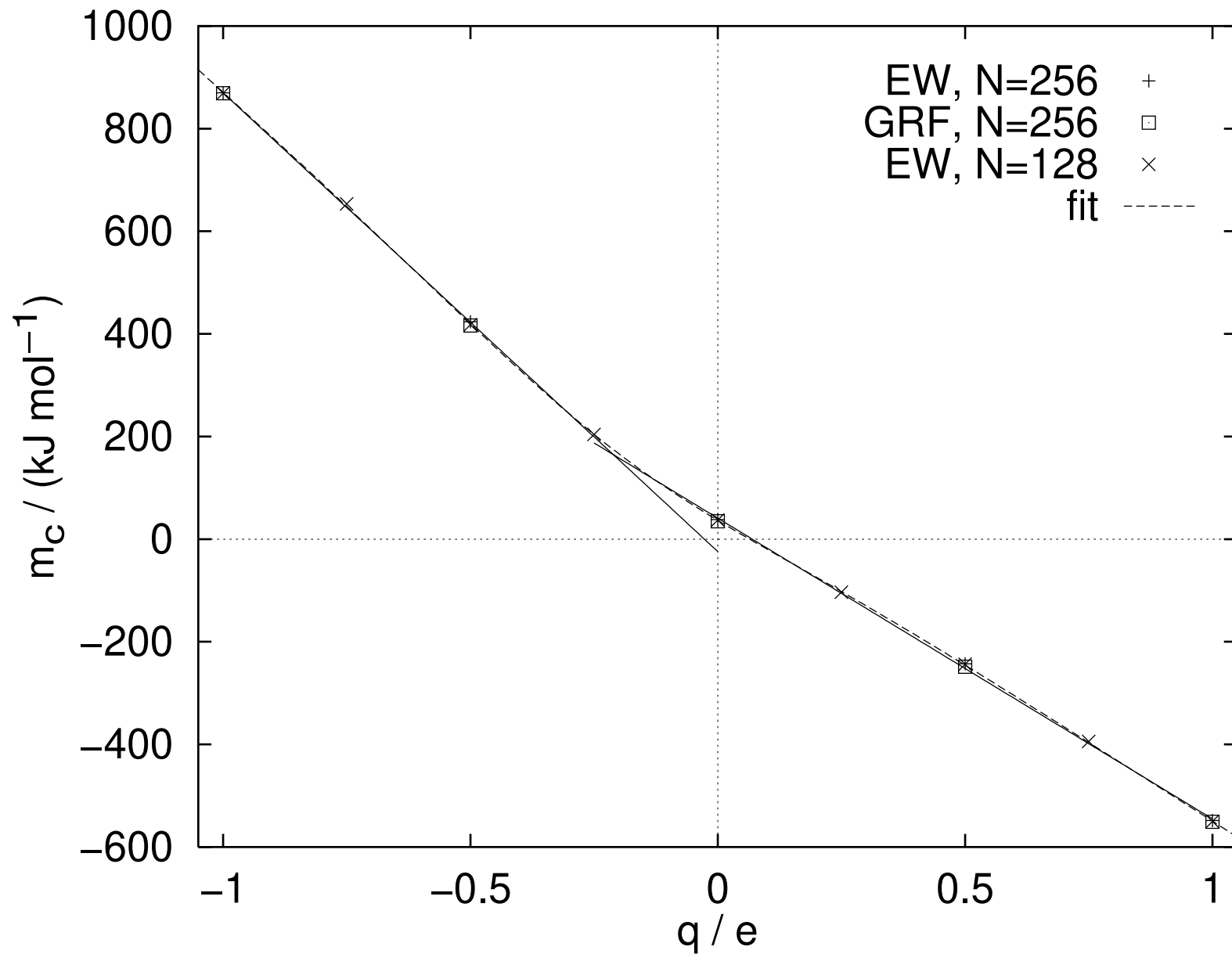


Fig. 3 (Hummer, Pratt, and Garcia)

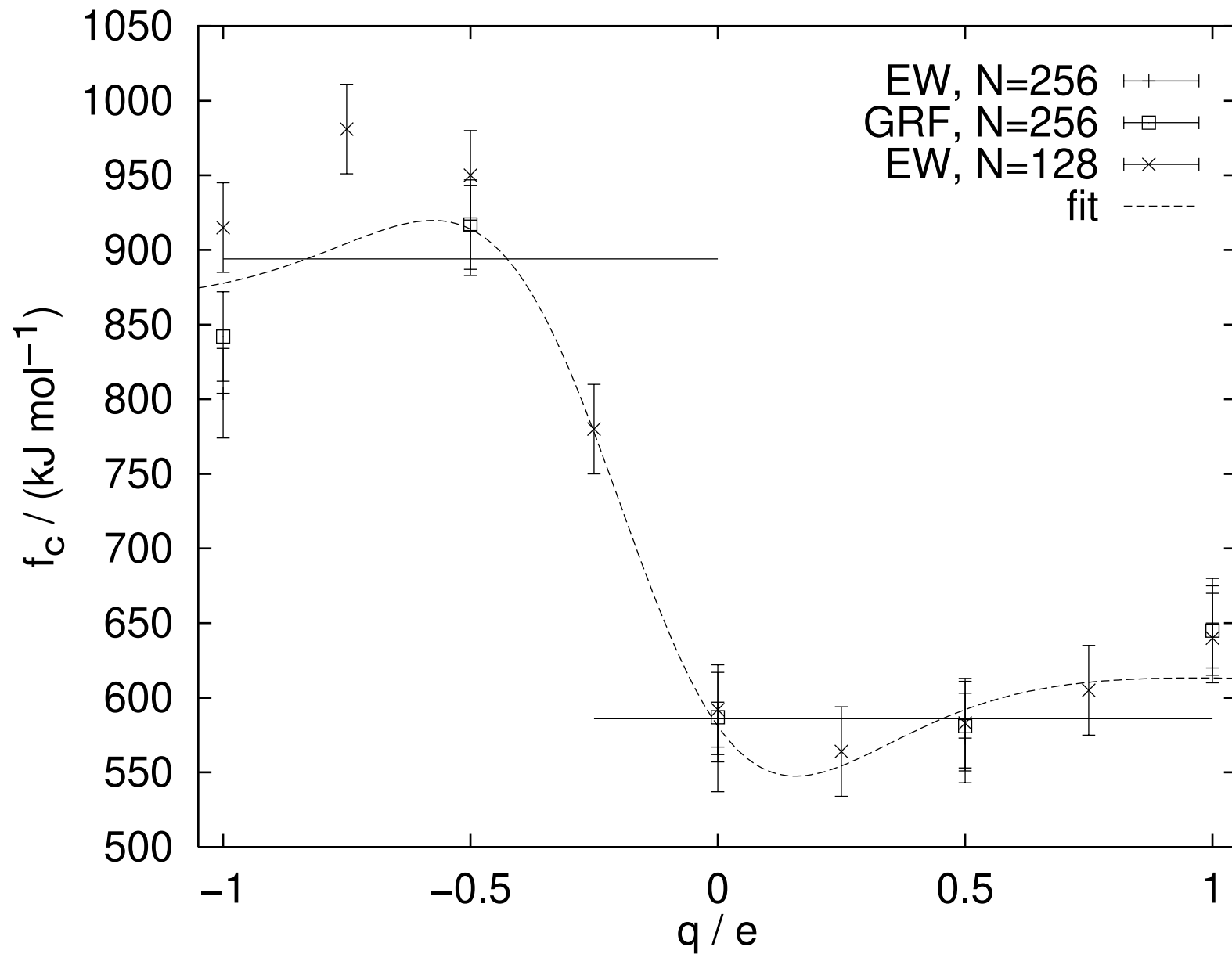


Fig. 4 (Hummer, Pratt, and Garcia)

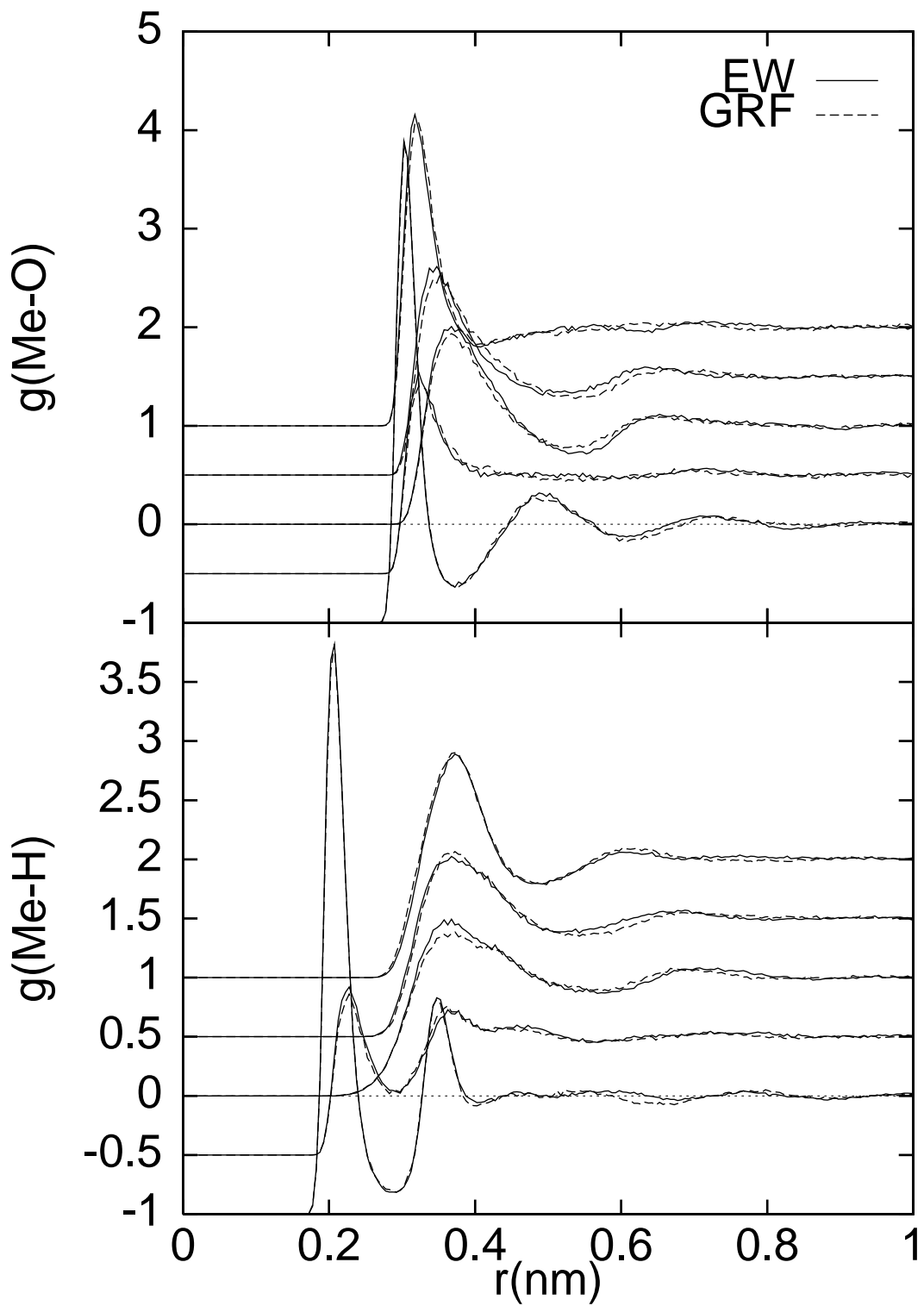


Fig. 5 (Hummer, Pratt, and Garcia)

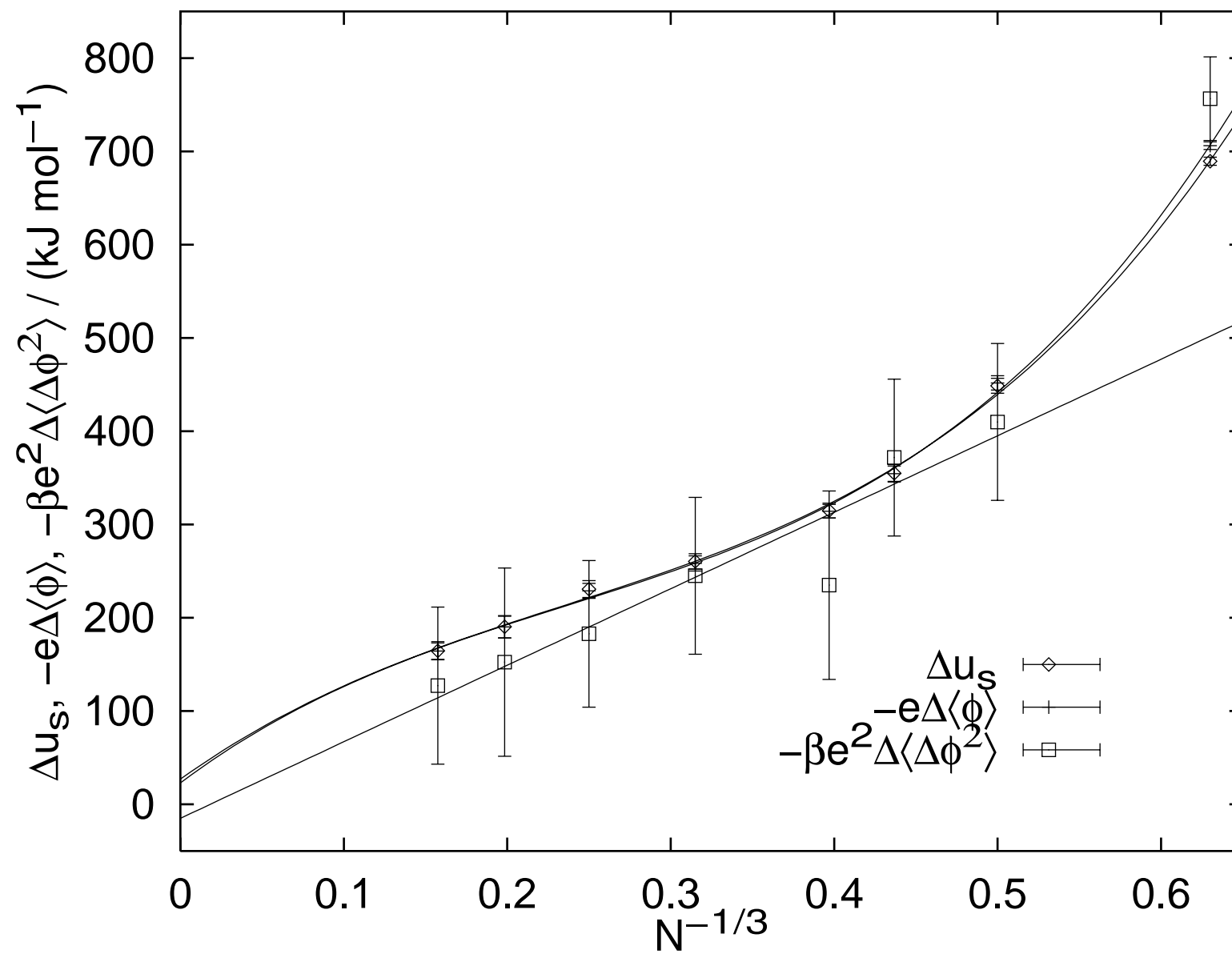


Fig. 6 (Hummer, Pratt, and Garcia)